Title
FLAME PROPAGATION, WALL HEAT TRANSFER, AND THEIR INTERACTION IN LEAN PREMIXED GASES

Author
Woodard, J.B.

Publication Date
1982

LBL-13950

Lawrence Berkeley Laboratory

UNIVERSITY OF CALIFORNIA

ENERGY & ENVIRONMENT DIVISION

To be presented at the Nineteenth International Symposium on Combustion, Technion-Israel Institute of Technology, Haifa, Israel, August 8-13, 1982

FLAME PROPAGATION, WALL HEAT TRANSFER, AND THEIR INTERACTION IN LEAN PREMIXED GASES

J.B. Woodard, D.H. Hirvo, R. Greif, and R.F. Sawyer

January 1982

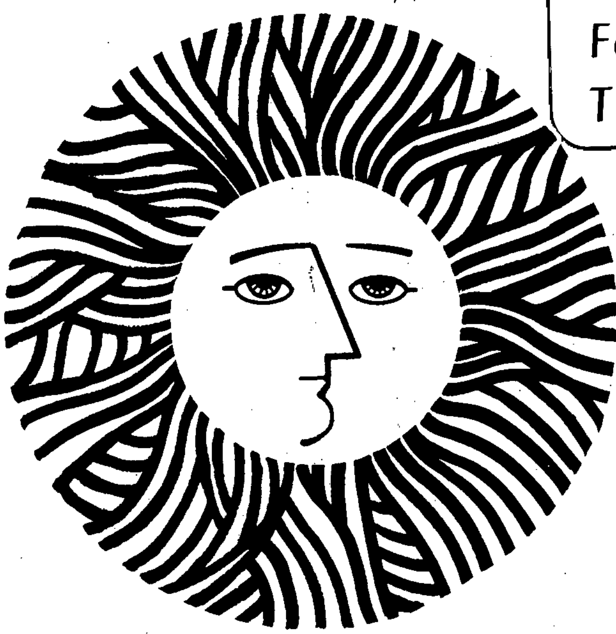

Prepared for the U.S. Department of Energy under Contract W-7405-ENG-48

DISCLAIMER

FLAME PROPAGATION, WALL HEAT TRANSFER, AND THEIR INTERACTION IN LEAN PREMIXED GASES

J.B. Woodard, D.H. Hirvo, R. Greif, and R.F. Sawyer

Department of Mechanical Engineering
and
Energy and Environment Division
Lawrence Berkeley Laboratory
University of California
Berkeley, CA 94720 USA

This work supported by the Assistant Secretary for Conservation and Renewable Energy, Office of Transportation Programs, Division of Transportation Energy Conservation of the U.S. Department of Energy under Contract W-7405-ENG-48.

ABSTRACT

Simultaneous data on single event flame propagation, wall heat transfer, and their interaction were obtained for a constant volume chamber. Pressure variation, wall temperature variation, and high speed schlieren movies were recorded for the combustion of methane and air for various equivalence ratios. Flame speed and wall heat flux variation with respect to time were calculated from the data. The results indicate that there are important geometry effects on flame speed due to side wall interaction. The wall heat flux data show effects due to the location of the flame relative to the location of the heat transfer measurement. Peak heat flux values occur when the flame front passes the location of measurement. High ignition energies are found to overdrive the rate of flame propagation.

INTRODUCTION

Premixed lean combustion in reciprocating engines offers the potential advantages of improved efficiency and reduced pollutant emissions. In the ideal limit, spark ignition gasoline engines could be operated in an unthrottled mode thereby providing advantages generally reserved to diesel engines. Recent work on lean burn engines may be found in a publication of the Institution of Mechanical Engineers[1]. Difficulties encountered in the application of lean combustion to engines include ignition reliability, flame speed reduction, increased cyclic variations, and increased hydrocarbon emissions as the lean limit is approached

This work is part of a larger study of fundamental processes important to homogeneous, premixed, lean burn engines, including ignition of very lean mixtures, flame propagation as the lean limit is approached, processes controlling hydrocarbon emissions, and wall heat transfer fundamentals. Experiments are conducted in unique compression-expansion devices incorporating square pistons and flat optical walls through which single combustion events may be observed from ignition through completion under conditions simulating reciprocating engine operation. Reported here are simultaneous, time resolved measurements of mean flame velocity and local heat transfer rates and coefficients. The interaction of the flame and wall heat transfer are thereby observed and the action of the wall to slow flame propagation and the flame to increase wall heat transfer are noted. Although constant volume, expansion, and compression-expansion conditions have been investigated, this paper is limited to the most thoroughly explored case, that of constant volume. Important related work includes the study of Andrews and Bradley of flame propagation as the lean limit is approached[3] and the studies of wall heat transfer in engines of Overbye, et al.[4] and Alkidas[5].

EXPERIMENTAL APPARATUS

The Compression Expansion Apparatus (CE-1) was designed to allow full optical access to combustion events simulating those occurring in reciprocating internal combustion engines. The test section consists of a horizontal duct with a 3.8 cm x 3.8 cm square cross section area. The test section is enclosed on both vertical sides by optical quality borosilicate glass windows and on one end by a movable, pneumatically driven aluminum piston. With the piston fully withdrawn, the test section has a total volume of approximately 216 cm^3. In this study, the test section served as a constant volume combustion chamber. The square cross section and glass sidewalls permit the use of schlieren photography to quantify the flame locations. The endwall opposite the piston contains the line ignition system consisting of a row of fifteen spark gaps. This row of electrodes is mounted in the test section running horizontally from window to window. This igniter was used to obtain flame uniformity in the direction perpendicular to the windows. The ignition system was operated at 46 kV with an ignition energy of approximately 260 mJ for most events. Variations in ignition energy, when they occur, will be noted.

There are four access ports on the test section to allow for the insertion of various instrumentation. These ports are located in the top and bottom steel sidewalls, at stations 0.5 cm and 13 cm from the ignition source endwall. A more detailed description of the experimental apparatus can be found in Oppenheim, et al.[6] and Smith[7].

In this study, simultaneous measurements of pressure, wall temperature, and flame front locations, all as a function of time, were made.

From these data, the temporal variation in flame speeds and wall heat flux during a combustion event were determined.

The combustion chamber pressure was measured using a piezoelectric transducer (AVL model 120P300CVK) located in the front access port just below the line ignition source. The calibration of the transducer was dynamically verified in the shock tube, and the observed rise time for the transducer ($\sim 10 \mu s$) was more than sufficient for our purposes.

The wall temperature gauge consists of a thin platinum film deposited on a glass ceramic base (Macor). The film acts as a resistance thermometer which is part of a Wheatstone bridge circuit. The platinum film resistance varies with changes in the film temperature, i.e. with the wall temperature. The response characteristic of the thin film gauge is of the order of a few microseconds. For calibration purposes and initial temperature measurement, a copper-constantan thermocouple is mounted on the surface. The dependence of the platinum film resistance on the surface temperature is determined by heating the gauge in an oven. The gauge calibration was found to be linear to within 1% over the temperature range of interest.

A premixed methane/air mixture flows through the test section through the back access ports. The equivalence ratio of the combustible mix was controlled by flow rotometers. The mixing device was calibrated using a Hewlett Packard Model 5750 Gas Chromatograph equipped with an Autolab System IV integrator. The uncertainty in the delivered equivalence ratio is approximately 1%.

The propagation of the two dimensional flame into the unburned fuel/air mixture was determined from high speed ($\sim$5400 frames per second) schlieren movies taken simultaneously with the chamber pressure and wall temperature data. Parallel light was provided from a light source, through the test section, through a vertical schlieren knife edge stop, and to the camera by the use of two spherical mirrors each with a focal length of 3.94 meters.

The pressure and wall temperature data were sampled by a PDP 11/34 mini-computer using an AR-11 analog to digital converter. The software written for data acquisition permits samples to be taken from both the temperature and pressure signals every 200μs.

ANALYSIS

Flame Speed

Flame speed with respect to the unburned gas was calculated from the pressure data and the location of the flame front as determined from high speed schlieren movies. The following assumptions were made:

(1) There is no net heat flux across the boundaries of the unburned volume.

(2) The flame front is considered to be negligibly thin and uniform in the horizontal direction perpendicular to the windows. It need not, however, be symmetric about the horizontal plane defined by the line ignition source.

(3) The unburned gas is assumed to behave as an inviscid ideal gas of constant specific heat ratio, γ_u. Its composition is that of the initial mixture.

(4) The pressure is assumed to be spatially uniform inside the combustion chamber.

In general, these assumptions are acceptable as shown by Smith[7].

The flame speed with respect to the unburned gas is defined by:

$$S_u = - \frac{\dot{m}_u}{\rho_u A_f} \qquad (1)$$

where $\dot{m}_u$ is the time rate of change of the unburned gas mass, ρ_u is the unburned gas density and A_f represents the area of the flame front. The first quantity may be expressed as follows:

$$\dot{m}_u = \frac{\partial}{\partial t} (\rho_u V_u) \qquad (2)$$

where V_u is the volume of the unburned gas remaining at any given time. Making this substitution into Eq. 1 and rearranging yields this relation:

$$S_u = -\frac{V_u}{A_f}\frac{\partial}{\partial t}\{\ \ell n(\rho_u V_u)\ \} \qquad (3)$$

From assumption 1), we have an isentropic process, $P^{1/\gamma_u}\rho_u^{-1}$ = constant giving:

$$\frac{1}{\rho_u}\frac{\partial \rho_u}{\partial t} = \frac{1}{P^{1/\gamma_u}}\frac{\partial P^{1/\gamma_u}}{\partial t} \qquad (4)$$

The expression for flame speed then can be reduced to:

$$S_u = -\frac{V_u}{A_f}\left[\ \frac{1}{\gamma_u P}\frac{\partial P}{\partial t} + \frac{1}{V_u}\frac{\partial V_u}{\partial t}\ \right] \qquad (5)$$

Wall Heat Flux

The wall heat flux is calculated from the transient wall temperature measurements. The time duration of the experiments is sufficiently small that the resistance wall temperature gauge can be considered to be thermally infinite (Fourier number $= \frac{\alpha t}{s^2} = 0.00087 << 1$). The one dimensional conduction equation in the solid is:

$$\frac{\partial T}{\partial t} = \alpha\frac{\partial^2 T}{\partial x^2} \qquad (6)$$

where X is the direction perpendicular to the wall surface, and the thermal diffusivity, $\alpha = \frac{k}{\rho c}$. The initial and boundary conditions are:

$$T(x,o) = T_i \tag{7a}$$

$$T(o,t) = T_w(t) \tag{7b}$$

$$T(\infty,t) = T_i \tag{7c}$$

The solution for this problem can be found using the solution for constant wall temperature and the Duhamel integral theorem as in Carslaw and Jaeger[8]. The results for the wall heat flux is given by:

$$q_w(t) = \sqrt{\frac{k\rho c}{\pi}} \left[\frac{T_w(t)-T_i}{\sqrt{t}} + \frac{1}{2} \int_o^t \frac{T_w(t)-T_w(\lambda)}{(t-\lambda)^{3/2}} \, d\lambda \right] \tag{8}$$

The values for the properties of Macor are:

$$k = 1.676 \text{ W/m K}, \quad \rho = 2520.02 \text{ kg/m}^3, \quad c = 460.55 \text{ J/kg K}$$

Thus the wall heat flux depends only on the wall temperature variation and the material properties k, ρ, and c.

RESULTS AND DISCUSSIONS

Pressures, wall temperatures, and schlieren movies were obtained simultaneously for a series of combustion events in which premixed methane and air were consumed in a constant volume process. With the temperature gauge located in the upper port near the igniter, data were obtained for equivalence ratios from 1.1 to 0.6[9]. In Figs. 1 and 2, pressure and wall temperature measurements for equivalence ratios of 1.0

Fig. 1 and 0.6, respectively, are shown. The pressure data exhibit a change

Fig. 2 of slope during the pressure rise which is thought to be a wall quenching effect as the flame contacts the cold steel side walls. This phenomenon was observed for all equivalence ratios. The wall temperature data show a very rapid initial rise, followed by a slower rise to the peak value. The sharp initial rise results from the passage of the flame near the wall temperature gauge, which for these cases is located near the igniter. Figures 3 and 4 show the locations of the flame front as a function of

Fig. 3 time for equivalence ratios of 1.0 and 0.6, respectively. These data

Fig. 4 were digitized from the high speed schlieren movies. The flame initially assumes an elongated shape, which then comes in contact with the steel side walls. For an equivalence ratio of 1.0 (Fig. 3) the flame maintains an approximate vertical shape with an instability near the centerline. In Fig. 4 for an equivalence ratio of 0.6, and therefore slower flame propagation, buoyancy forces cause the burnt gases, which are hotter than the unburnt gases in front of the flame, to rise. The flame, as a result, assumes a sloping profile.

From these experimental measurements, the temporal variation in wall

Fig. 5 heat flux and in flame speed were calculated. In Fig. 5, the wall heat flux variations for equivalence ratios of 1.0 and 0.6 are shown. In general, the heat flux exhibits two major peaks; although in the lean case (equivalence ratio of 0.6) the second peak is less significant.

As previously discussed, the initial rise in the heat flux results from the flame passing the wall temperature gauge which is located on the side wall near the igniter. The variation of wall heat flux with respect to location was also studied and is discussed later. A less pronounced third peak in the heat flux is sometimes observed and is attributed to run to run variations in flame shape and propagation.

The temporal variations of the flame speed at equivalence ratios of

Fig. 6 1.0 and 0.6 are shown in Fig. 6. The symbols on the graph represent actual data points; a smoothing cubic spline is also shown. In general, for all equivalence ratios considered, the flame speed has two major peaks. For the equivalence ratio of 0.6, these peaks are much less pronounced. The sharp dip in the flame speed that is present between the two peaks is found to coincide with the point on the pressure curve where the slope changes. These phenomena result from quenching of the flame due to interaction with the cold side walls. It should be noted that for the higher equivalence ratios; eg., 1.0, the relatively high ignition energy of 262 mJ, may be overdriving the flame as shown by de Soete[10]. The effect of decreasing the ignition energy was also studied and will be discussed later.

The effect of temperature gauge location on wall heat flux was analyzed by obtaining measurements of temperature in the various instrumentation ports in the apparatus. The wall heat flux calculated from these wall

Fig. 7 temperature measurements is shown in Fig. 7. For an equivalence ratio of 1.0, the heat flux is shown for the upper ports both near and far from the igniter. For the upper port far from the igniter, the steep rise in heat flux occurs much later, and there is only one maximum. For an equivalence ratio of 0.6, the heat fluxes for ports near and far from the igniter are shown in Fig. 7. For the upper port far from the igniter the rise in heat flux occurs about 175 ms later than for the upper port near the igniter. For the lower port far from the igniter, the speed of the flame and buoyancy both have an effect on the heat flux. Since the flame assumes a more horizontal orientation, as shown in Fig. 4, the lower temperature gauge detects the flame much later. There is approximately a 180 ms difference in the time of the heat flux rise between the upper and lower ports far from the igniter.

Figure 8 shows the effect of varying the ignition energy on the measured flame speeds. Curve A is the flame speed for an ignition energy of 261.8 mJ; curve B, for 159.0 mJ; and curve C, for 57.5 mJ. For higher ignition energies, the overall rate of consumption of fuel and oxidizer is increased, as shown by the decrease in time required for the lower ignition energy flames (curves B and C) to reach completion. The surprising high peak flame speed for an ignition energy of 57.5 mJ is the result of a smaller flame kernel for the smallest ignition energy (the A_f^{-1} term dominates in the mean flame speed calculation, Eg. 5). The overall energy release rate, as reflected in the rate of pressure rise, increases with increasing ignition energy.

CONCLUSIONS

Simultaneous data on single event flame propagation, wall heat flux, and their interaction were obtained. Pressure variation, wall temperature variation, and high speed schlieren movies were recorded for constant volume combustion of methane and air for a series of equivalence ratios. The flame speed and wall heat flux variations with time were calculated from the data. The results indicate that there are important geometry effects on the flame speed due to side wall interaction. The wall heat flux data show effects due to flame location relative to the location of the heat transfer measurement. Peak heat flux values coincide with flame passage near the temperature gauge. To further investigate this flame location effect on heat flux, wall temperatures were obtained for three temperature gauge locations. These data indicate that the speed of the flame and buoyancy both have an effect on the heat flux. Data were also obtained to study the effect of ignition energy on flame speed. High ignition energy reduces the time required for completion of combustion.

SYMBOLS

A	Area
c	Heat Capacity
k	Thermal Conductivity
m	Mass
P	Pressure
q	Heat Flux
S	Flame Speed
T	Temperature
t	Time
V	Volume
x	Direction Normal to Sidewall
α	Thermal Diffusivity
γ	Ratio of Specific Heats (= c_p/c_v)
η	Dummy Variable of Integration
λ	Dummy Variable of Integration
ρ	Mass Density

SUBSCRIPTS

f	Flame
i	Initial
p	Constant Pressure
u	Unburned
v	Constant-Volume
w	Wall

SUPERSCRIPTS

	Time Rate of Change

ACKNOWLEDGEMENTS

The authors appreciate the assistance of K. Hom, H. Stewart, R. Jensen, and W. Pitz in the preparation of the experimental apparatus and conduct of the experiment. G. Hubbard wrote the data logging software and provided invaluable assistance in coupling the experiment and PDP 11/34 computer. Sandia National Laboratories Livermore provided computational facilities, graphics equipment, and support under their doctoral study program for JBW.

This work supported by the Assistant Secretary for Conservation and Renewable Energy, Office of Transportation Programs, Division of Transportation Energy Conservation of the U.S. Department of Energy under Contract W-7405-ENG-48.

REFERENCES

1. Institute of Mechanical Engineers: Conference Publication 1979-9, Fuel Economy and Emissions of Lean Burn Engines,

2. Noguchi, M., Sanda, S. and Nakumura, N.: Development of Toyota Lean Burn Engine, SAE Paper No. 760757, 1976.

3. Andrews, G.E. and Bradley, D.: Combustion and Flame, 19, 275 (1972).

4. Overbye, V.D., Bennethum, J.E., Uychara, O.A. and Myers, P.S.: Unsteady Heat Transfer in Engines, Trans. SAE 69.

5. Alkidas, A.C.: Heat Transfer Characteristics of a Spark-ignition Engine, Joint ASME/AIChE 18th National Heat Transfer Conference, San Diego, CA, ASME Paper No. 79-HT-76, August 6-8, 1979.

6. Oppenheim, A.K., Cheng, R.K., Teichman, K., Smith, O.I., Sawyer, R.F., Hom, K., and Stewart, H.E.: A Cinematographic Study of Combustion in an Enclosure Fitted with a Reciprocating Piston. Paper presented at the Conference on Stratified Charge Engines, London, November 23-24, 1976.

7. Smith, O.I.: Lean Limit Combustion in an Expanding Chamber, Seventeenth Symposium (International) on Combustion, p. 1305, The Combustion Institute, 1979; and Ph.D. Thesis, University of California, Berkeley; also available as LBL Report No. 6851, 1977.

8. Carslaw, H.S., and Jaeger, J.C.: Conduction of Heat in Solids, Oxford University Press, Oxford, 1978.

9. Woodard, J.B., Hirvo, D.H., Greif, R., and Sawyer, R.F.: Wall Heat Transfer and Flame Propagation in a Constant Volume Duct, Paper No. WSCI 81-51 presented at the Western States Section/The Combustion Institute Fall Meeting, Tempe, AZ, October 19-20, 1981; also LBL Report No. 13021.

10. de Soete, G.G.: Measurement of Initial Flame Speed by Laser Tomography. First Specalists Meeting (International) of the Combustion Institute. Bordeaux, France, July 20-24, 1981.

Figure 1

Absolute pressure and wall temperature variation with time; constant volume combustion, equivalence ratio 1.0.

Figure 2

Absolute pressure and wall temperature variation with time; constant volume combustion; equivalence ratio 0.6.

Figure 3

Flame front location from schlieren movies for time steps of 3.74 ms starting at ignition; total elapsed time to last location shown is 56.1 ms; equivalence ratio 1.0.

Figure 4

Flame front location from schlieren movies for time steps of 14.17 ms starting at ignition; total elapsed time to last location shown is 283.4 ms; equivalence ratio 0.6.

Figure 5

Wall heat flux variation with time at upper port near igniter; constant volume combustion; equivalence ratio 1.0 and 0.6.

Figure 6

Flame speed variation with time; constant volume combustion; equivalence ratios 1.0 and 0.6.

Figure 7

Wall heat flux variation with time for three locations in apparatus: A) upper port near igniter, B) upper port far from igniter, C) bottom port far from igniter; constant volume combustion; equivalence ratios 1.0 and 0.6.

Figure 8

Flame speed variation with time for three ignition energies: A) 262 mJ, B) 159 mJ, C) 57.5 mJ; constant volume combustion; equivalence ratio 0.8.

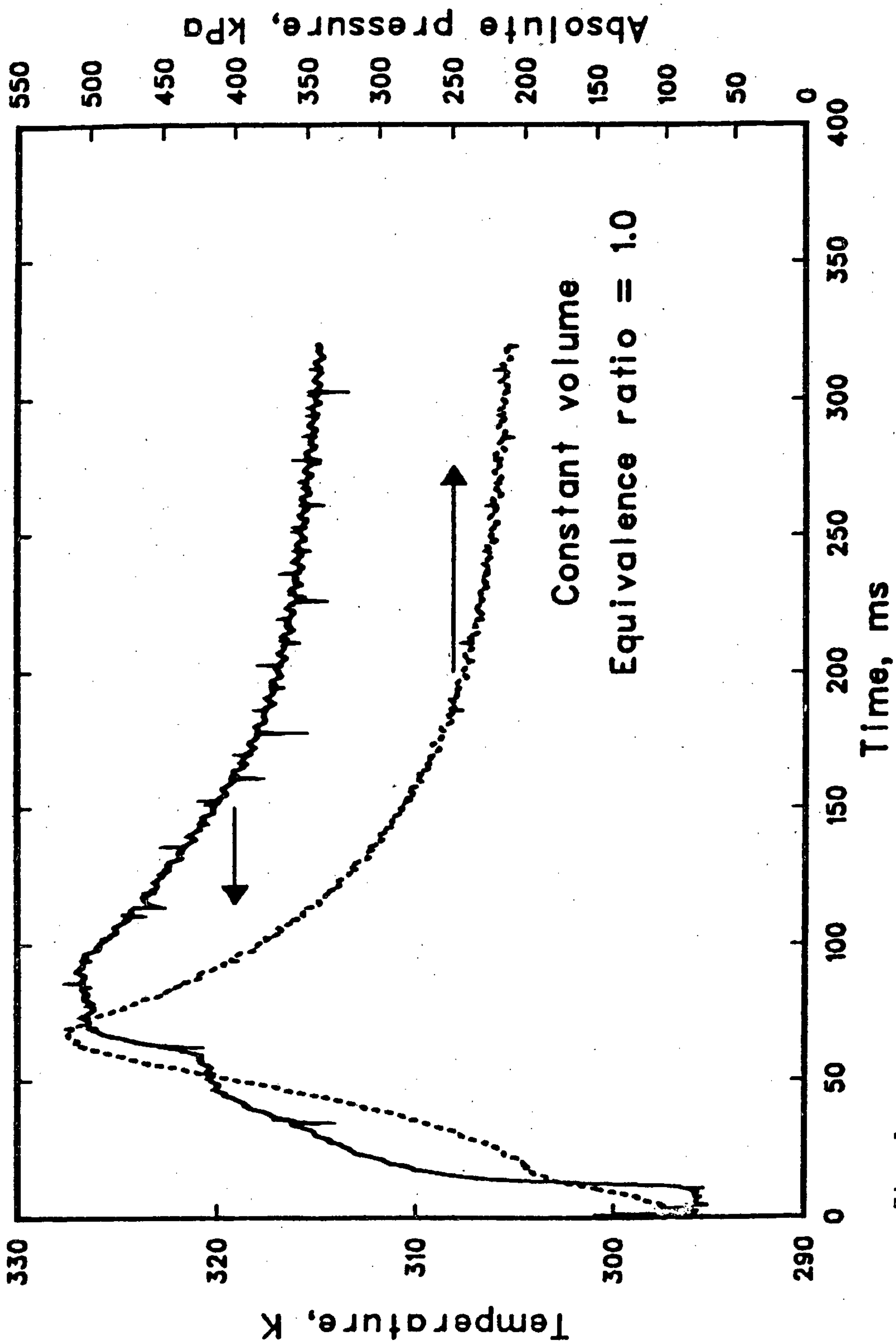
Absolute pressure, kPa
550
500
450
400
350
300
250
200
150
100
50
0
Temperature, K
330
320
310
300
290
Time, ms
0
50
100
150
200
250
300
350
400
Constant volume
Equivalence ratio = 1.0

Fig. 1

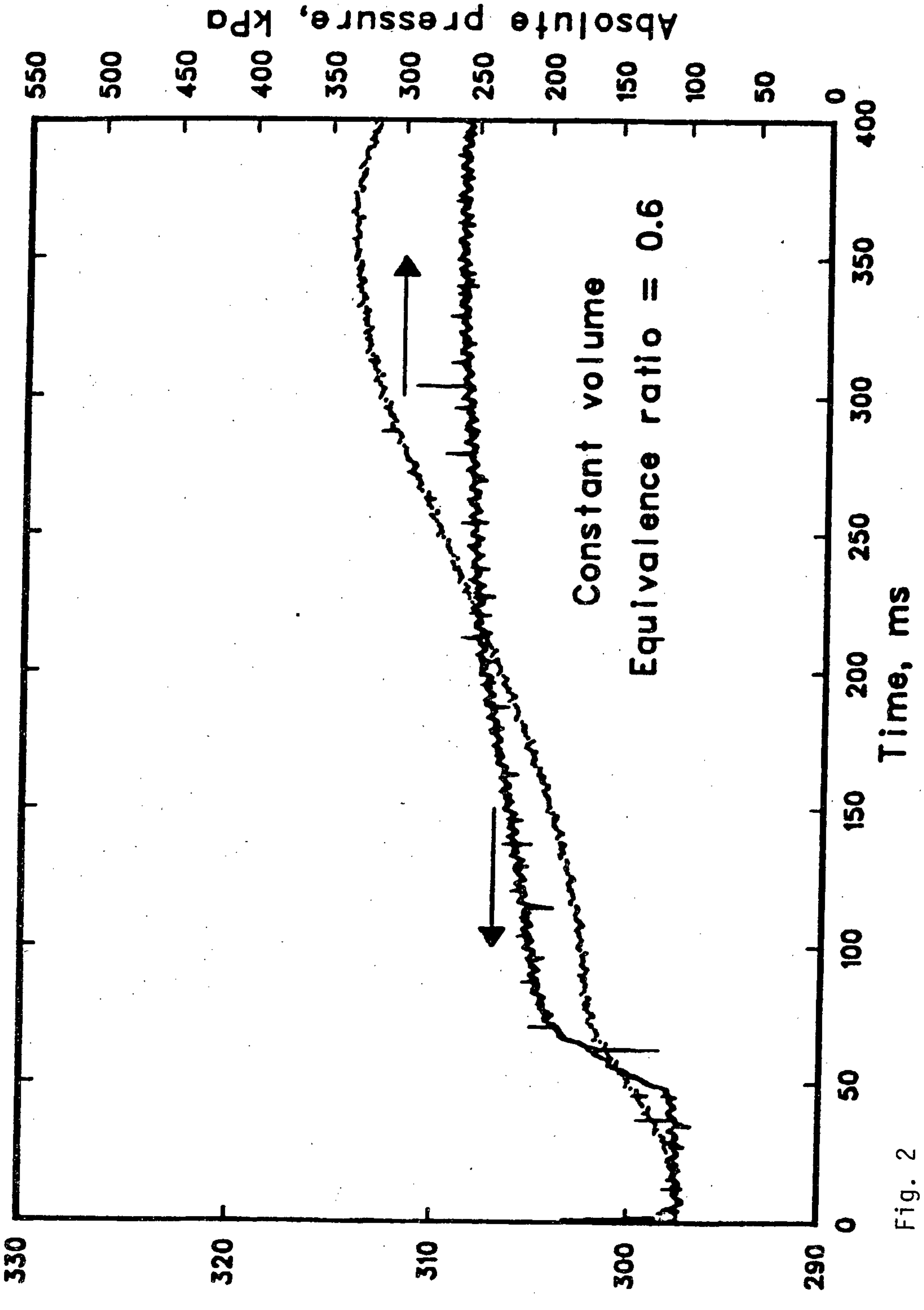
Absolute pressure, kPa
0
50
100
150
200
250
300
350
400
450
500
550
Temperature, K
290
300
310
320
330
Time, ms
0
50
100
150
200
250
300
350
400
Constant volume
Equivalence ratio = 0.6

Fig. 2

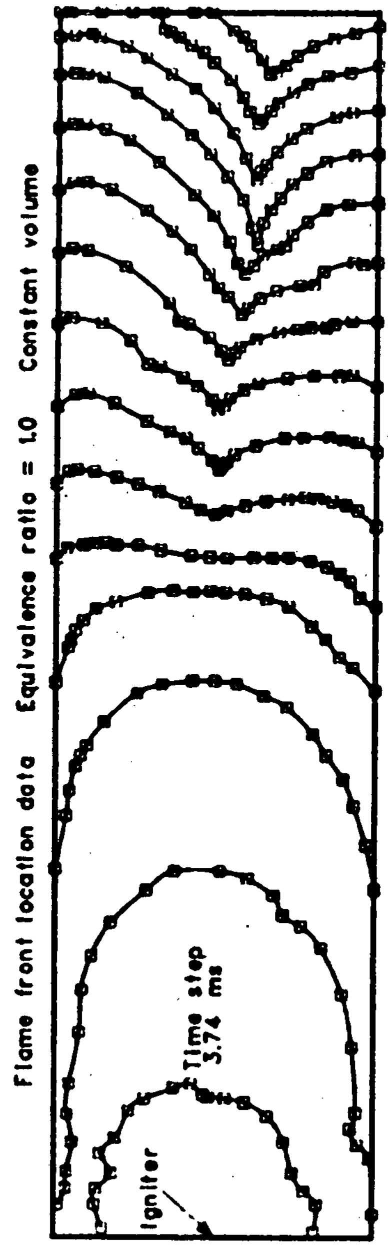
Flame front location data Equivalence ratio = 1.0 Constant volume
Time step
3.74 ms
Igniter

Fig. 3

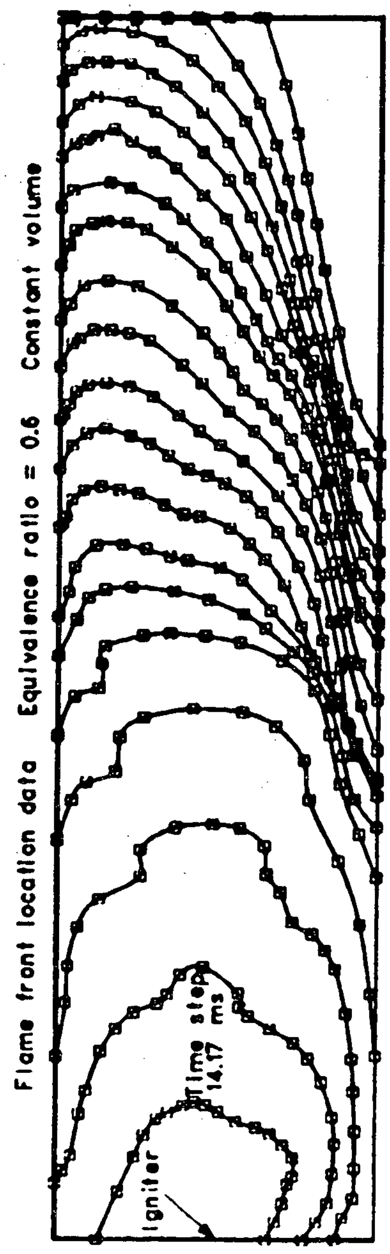
Flame front location data Equivalence ratio = 0.6 Constant volume
Igniter
Time step 14.17 ms

Fig. 4

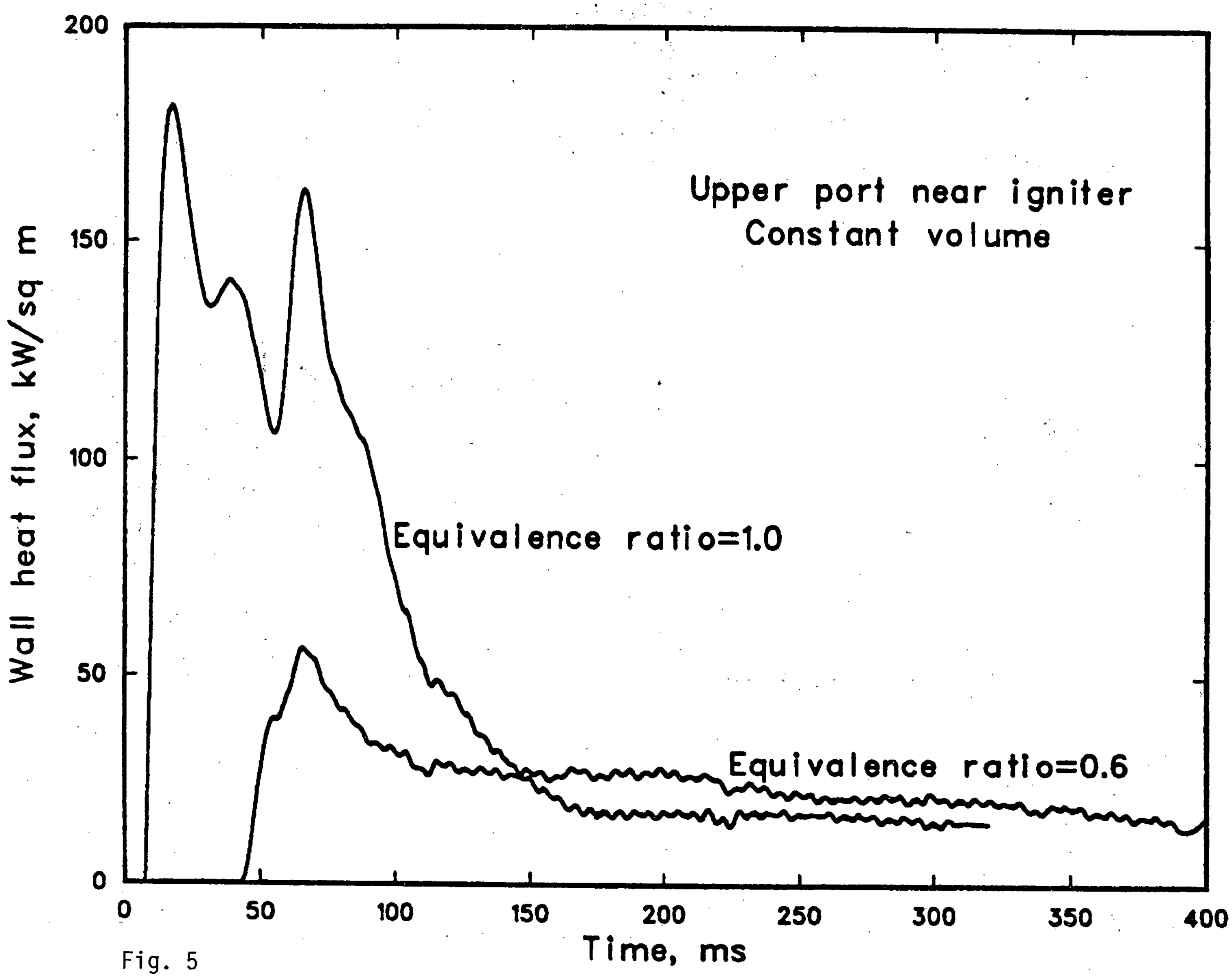
Upper port near igniter
Constant volume
Equivalence ratio=1.0
Equivalence ratio=0.6
Wall heat flux, kW/sq m
Time, ms
0
50
100
150
200
250
300
350
400

Fig. 5

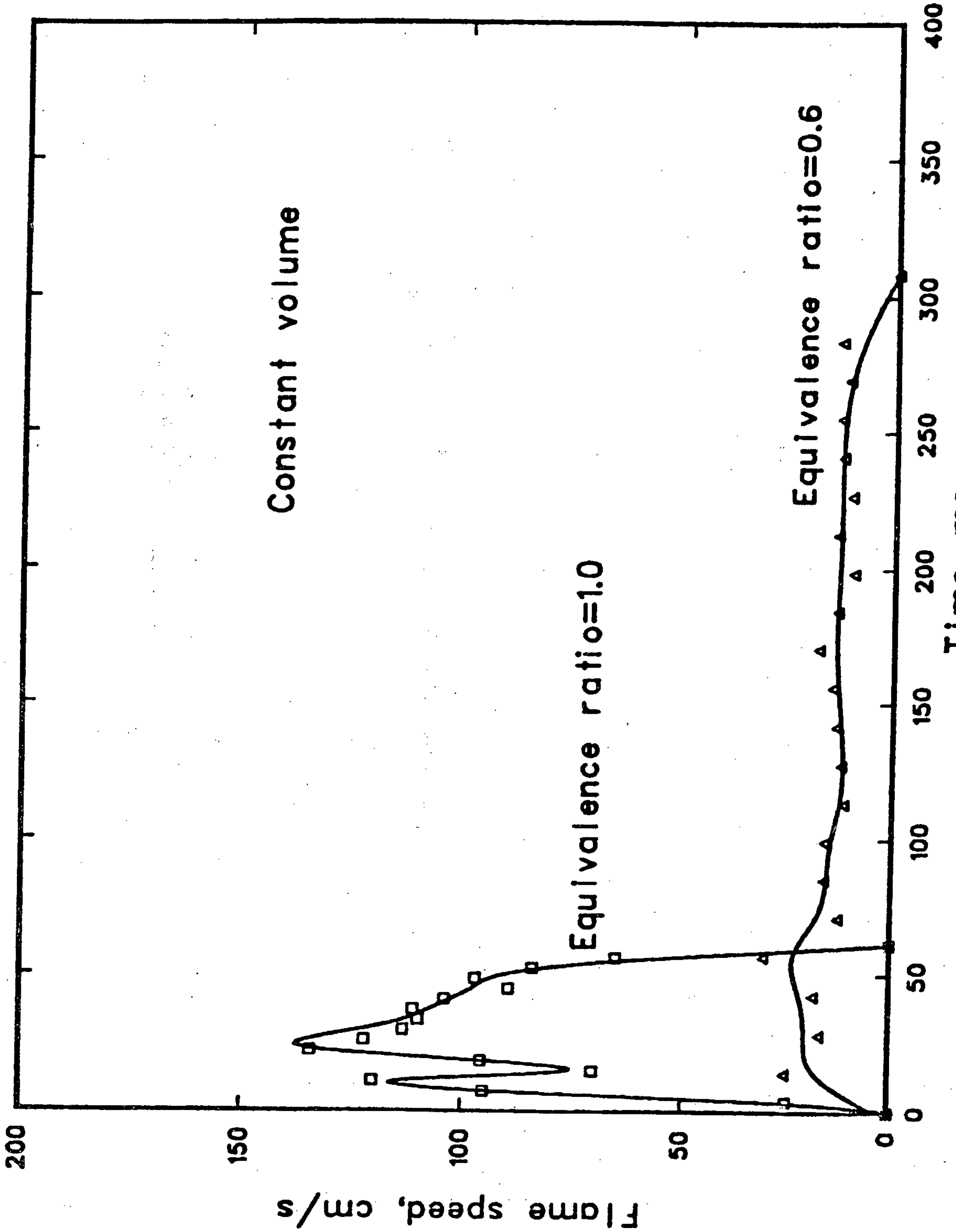
Constant volume
Equivalence ratio=1.0
Equivalence ratio=0.6
Time, ms
Flame speed, cm/s
0
50
100
150
200
250
300
350
400

Fig. 6

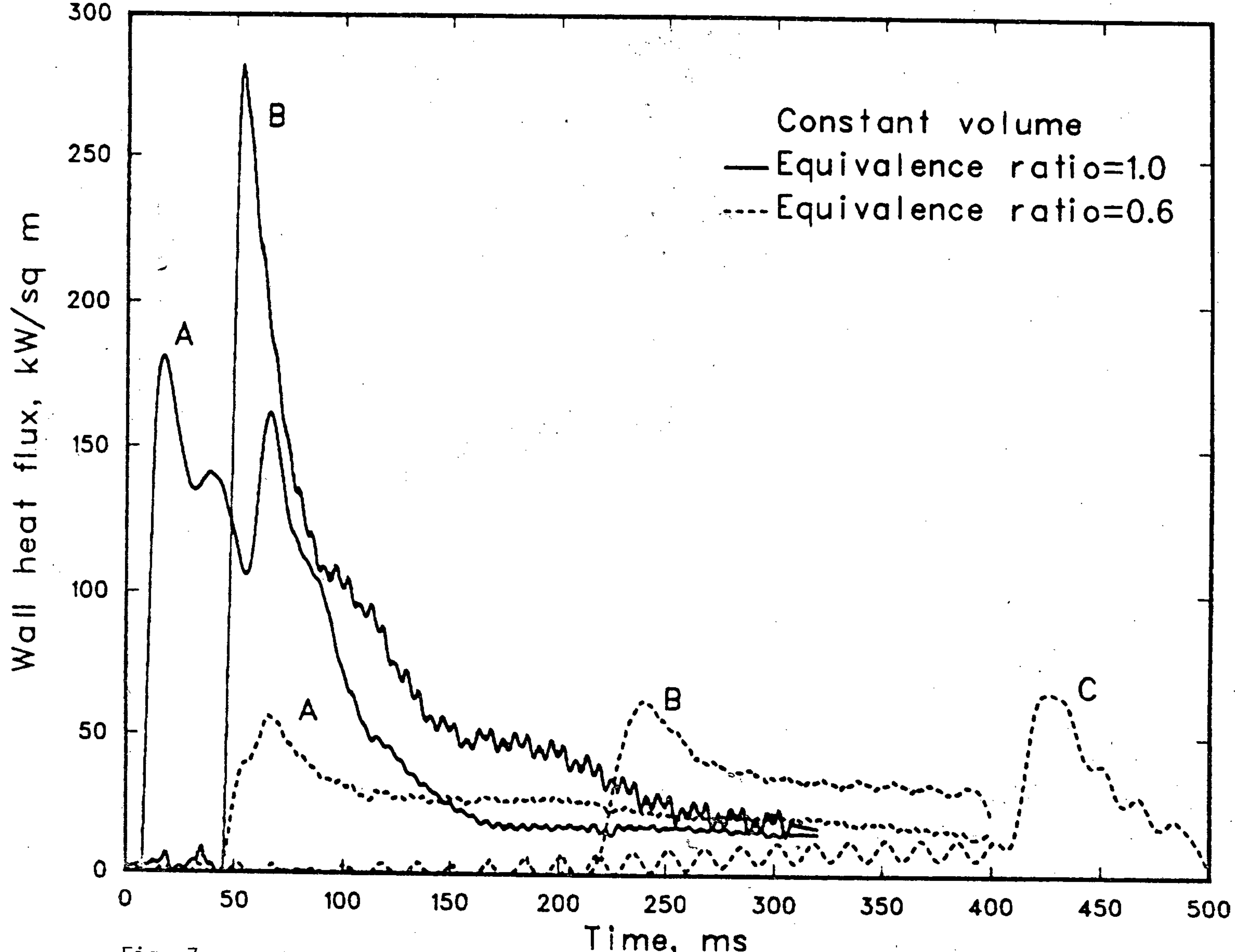
Constant volume
Equivalence ratio=1.0
Equivalence ratio=0.6
A
B
A
B
C
Wall heat flux, kW/sq m
Time, ms
0
50
100
150
200
250
300
350
400
450
500

Fig. 7

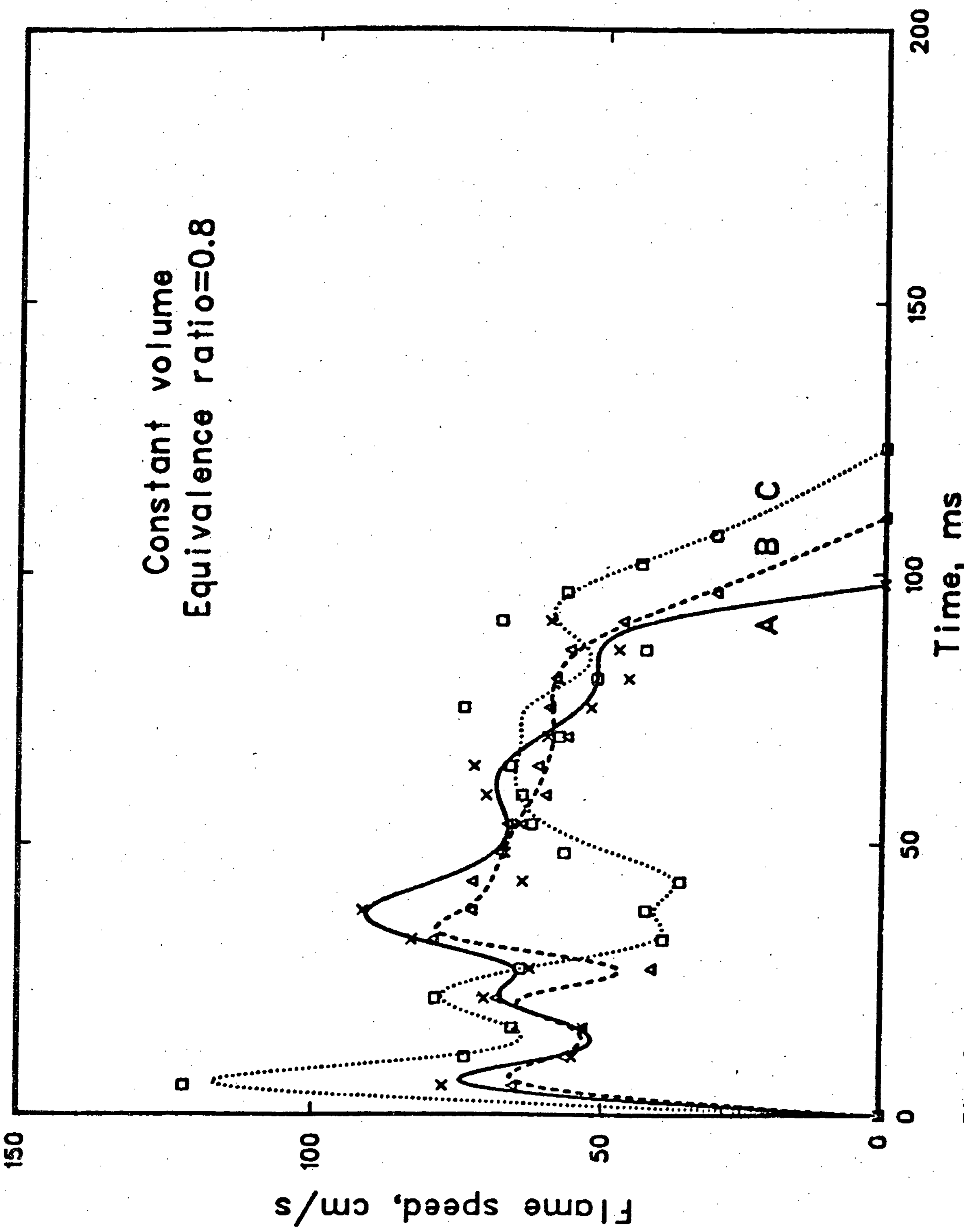
Constant volume
Equivalence ratio=0.8
A
B
C
Time, ms
Flame speed, cm/s
0
50
100
150
200
0
50
100
150

Fig. 8

TECHNICAL INFORMATION DEPARTMENT
LAWRENCE BERKELEY LABORATORY
UNIVERSITY OF CALIFORNIA
BERKELEY, CALIFORNIA 94720